Clinical Applications of Dual Energy Computed Tomography: Focus on Neuroimaging, Uric Acid Stones and Liver Diseases

Musaib Rather[1], Goswami Nidhi[2]
[1,2]*Chitkara University, Chandigarh, India*

Abstract—**The Dual Energy Computed Tomography (DECT) technology is widely used for many fields of medical study. Recent advancements in computed tomography have made it possible to acquire and analyze X-rays simultaneously with two distinct amounts of energy (high and low), creating new opportunities for neurological research and development. Tumors exhibit a greater contrast-to-noise ratio (CNR) than liver tissue, therefore using both high and low tube potentials to create blended images during DECT, which in turn can aid in the diagnosis of cancer. By raising the CNR and signal-to-noise ratio and lowering hardening of the beam, the use of contrast agents enhances image quality. The identification and characterization of hepatic anomalies, such as mass lesions, can be enhanced by DECT. The many uses of DECT in imaging of the liver are outlined and shown in this research. Uric acid stones can also be diagnosed using this technique. In addition, increased detection of aneurysms, vascular malformations, and iodine enhancement within a single scan in DECT in neuroimaging is made possible by bone elimination, material description, and monoenergetic reconstructions. Monoenergetic reconstructions allow for enhanced iodine attenuation and/or improved quality of brain and spine imaging. This review summarizes the numerous operations of DECT in liver imaging, application of DECT in neuroimaging and the determination of ailments such uric acid stones and liver problems. There is also a brief analysis on DECT's future possibilities.**

Index Terms—**DECT, X Ray, Neuroimaging, Disease detection, SNR, CNR**

I. INTRODUCTION

The DECT system consists of a single gantry with two x-ray tubes positioned orthogonally at 90° angles (Fig. 1). Two x-ray tubes or two photon spectra are used as the photon source in dual energy computed tomography, or "DECT." It is also named as spectral computed tomography. To acquire separate absorption measurements in the spectrum using standard CT detectors, two photon spectra are now produced by either varying the voltage of one x-ray tube or switching the voltage of both tubes [1].

The spinning anodes of polychromatic spectra, which are employed in DECT diagnostic imaging tubes, have a characteristic tungsten material lining and are superimposed on a continuous spectrum of bremsstrahlung. As a result, DECT has two x-ray spectra rather than two separate energies. The X-ray tubes use revolving anodes with polychromatic spectra, which are made up of tungsten anode characteristic lines overlaid over a continuous bremsstrahlung spectrum. They are employed because their quanta output is adequate for diagnostic imaging. Thus, two photon spectra are employed rather than two different photon energies in DECT.

The voltage that is supplied determines the maximum photon energy. Nonetheless, the mean photon energies are significantly lower than the maximum energy, and the disparity between them is less than anticipated. The average photon energies are around 76 keV and 56 keV, respectively, while employing 140 kV and 80 kV and standard filters. To make sure that the two tubes produce identical amounts of photons when utilized independently, the tube current should be adjusted. Typically, 80 and 140 kV settings are employed because they offer the greatest variation and the least amount of spectrum overlap when using conventional tubes [1].

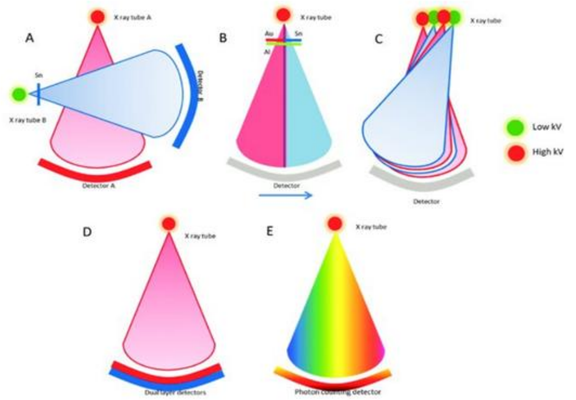

Figure 1: Dual-energy computed tomography (DECT) methods are shown. (A) DECT using two sources. Two 90° orthogonally positioned X-ray tubes with matching detectors have distinct tube potentials. (B)Dual beam filtration, a single X-ray source that is positioned along the Z-axis with two distinct filters. (C) Quick kilovolt transitions. In less than 0.2 milliseconds, the X-ray tube quickly transitions from the low to the high voltage during a single gantry spin. (D) A two-layer sensor. a sandwiched or stacked detector and a single source. (E) Devices for counting photons.

The tissue characteristics and contrast medium employed in DECT are significant additional factors. In DECT, differentiation is carried out based on the tissue's or the contrast medium's spectral characteristics, which allow for differentiation based on x-ray attenuation at various photon energies. Nonetheless, the photoelectric effect, coherent scatter, and Compton effect are responsible for the x-ray attenuation. Because the photoelectric effect is proportionate to the atomic number, it depends on the atomic number among these features. Except for calcium and magnesium, the majority of atoms in the human body have a weak photoelectric effect; in contrast, contrast media has a relatively powerful photoelectric effect. Photons interact with the atom's K shell to produce these variations. As the atomic number increases (55-cesium), the photoelectric effect increases as well. Due to their increased photoelectric effect and larger atomic number, contrast materials such as iodine (53), xenon (54) and barium (56), are utilized. Spectral behavior in DECT aids in the distinction between various tissues. Techniques like as quantum-counting detectors, fast voltage changing, DSCT, layer detectors, and sequential acquisition are technically sound. DECT provides the ability to use spectrum data for diagnostic applications. The technological methods, which vary in their inherent benefits and drawbacks, particularly with regard to dose efficiency and spectral contrast [1,2,3,4,5,6]. As previously explained, DECT has a wide range of uses, particularly in neuroimaging and illness detection. This paper presents a critical assessment of the use of DECT with an emphasis on neuroimaging and the diagnosis of conditions such as, liver illness, and uric acid stones.

II. AREAS OF APPLICATION

DECT has immense applications in disease detection and also in various imaging techniques. Following sections present a critical review of the application of DECT focusing on neuroimaging and detection of diseases like uric acid stones and liver diseases.

a) Neuroimaging

The usage of CT has increased with the incorporation of tissue characterization using DECT. Prior to the introduction of CT in 1971, neuroscience relied on indirect methods such as X-rays and myelography. Whole-body screening was first limited to brain imaging due to long acquisition periods, but by 1974, developments in technology had allowed for important diagnostic uses, including the identification of syringomyelia [7, 8]. Later advancements in spatial detail, such multidetector-row CT (MDCT) and helical acquisition, allowed for more advanced applications, including 3D imaging, active ("4D") imaging, and brain perfusion [9–12]. Systems like Siemens, GE, and Phillips' DECT systems, which assess energy-dependent attenuation, enable material discrimination. This facilitates the distinction between substances, including iodine and bleeding, that seem to be same on conventional CT [13–18]. In neuroradiology, DECT is starting to gain traction for applications such as iodine mapping, bone excision in CT venography (CTV) especially CT angiography (CTA), and digital non-contrast imaging to detect current bleeds in stroke patients [19]. Differentiating between blood and iodine is useful for managing high-density lesions, delivering contrast media, or performing intra-arterial re Canalization in stroke patients. Spot symptoms and the identification of underlying medical conditions, both vascular and non-vascular, may be useful for patient intracranial bleeding [20]. DECT is coming up to other imaging subspecialties in neuroimaging. The field of neuroimaging is growing in popularity, and its benefits are understood. This, as the ambiguous 4th factor in 3-material decay, necessitates both the resolution of DECT's limitations and the further development of DECT techniques and applications in brain imaging. Recent work has revealed advanced monoenergetic reconstructions that combine the privileges of lower and higher keV reformation by employing only a piece from their range of frequency. It is potent to raise the bar for monoenergetic reconstructions. Monoenergetic image formation, a utilization of DECT, and material characterization, along with bone removal, provide improved identification of vascular malformations, iodine enhancement, and aneurysms within a single scan [20].

b) Uric acid stones

Excess or elevated uric acid levels in the urine cause crystallization, which is the cause of uric acid stones, a kind of nephrolithiasis. Urinary tract infections (UTIs), urinary obstructions, and in certain situations, renal failure can result from the presence of urinary stones if treatment is neglected. Therefore, in order to manage and prevent uric acid stones, it is important to completely comprehend their occurrence and etiology. Since DECT can distinguish between different stones by assessing their composition by measuring the amount of x-ray attenuation by the stones, it has emerged as a useful method or instrument for the detection of uric acid stones in the modern day. The information regarding the quantity of stone composition that DECT offers is very helpful in selecting an appropriate treatment strategy. Recent research indicates that while DECT is completely undetectable on traditional x-rays, it can effectively identify urinary stones.

Very few research has incorporated mixed stones; the majority of investigations present, concentrated on pure stones. Graser et al. [21] used an initial generation dual-source scanner functioning at 80kV and 140kV to study the distinction of stone composition. Four mixed stones were included in their analysis, although the majority of the stones were pure stones. More mixed stones as well as pure UA and non-UA stone samples were used in the study by Boll et al. [22]. The primary objective was to distinguish between pure UA, pure non-Uric Acid, and mixed stones, and every single stone was handled as a whole. Consequently, constituent elements within the blended stones lacked both differentiation and quantification. Color coding in conjunction with commercial DECT software was utilized by Stolzmann et al. [23, 24] to identify Uric acid and non-Uric acid components in pure and blended stones. If any red is seen, stones were deemed to have Uric acid; if any blue is seen, they were deemed to have non-Uric acid materials. Pixel-by-pixel dual-energy analysis was carried out by Shuail L et al. [25].

Every stone's UA or non-UA status was established by contrasting its CT number percentage to a preset baseline. When second-generation dual-source scanners were equipped with a tin filter and the 100-kV/Sn140-kV scan mode became available, DECT performance on large patients improved. On the third version of the dual-source scanner used in this experiment, tin filters were present in four of the five dual-energy scanning modes on the high (150 kV) beam. By using phantoms that approximated adult patients with lateral widths that varied between 30 to 55 cm, indicating lean to highly obese, a wide range of physical sizes were covered in this investigation. To choose whichever dual-energy scan methods to use, they employed phantom sizes: Since these modes provide improved spectral separation although still allowing for appropriate penetration for humans in this size range, 70 and 80 kV were used, respectively, for the specters portraying fine and average patients. For phantoms (specters) that resembled tall and obese patients, respectively, they used 90 and 100 kV to guarantee adequate penetration. The ability of DECT to perfectly scale both the UA and non-UA constituents of mixed urinary stones was therefore investigated.

c) Liver diseases

Liver iron measurement is crucial for assessing iron overload conditions, which can lead to cirrhosis, hepatocellular carcinoma, and the death of liver cells. Liver biopsy is considered to be a metric for determining liver concentration of iron (LIC), has been used historically. However, biopsies are invasive and unsuitable for routine observation. MRI has become the accepted norm for non-invasive LIC assessment because it is so accurate at tracking iron-reducing medications and staging iron overload [26, 27, 28]. One of the many MRI methods that have been extensively utilized to determine iron level is T2* relaxometry, a reliable non-invasive option to biopsy [29]. Dual-energy CT (DECT) measurements of liver iron have been attempted since the 1980s. DECT has the advantage of separating materials dependent on energy attenuation, making it possible to separate substances like iron and fat. Numerous studies, particularly in live animal models and non-living phantom tests, have examined the potential benefits of DECT throughout this arena [30, 31, 32]. Luo et al. [34] demonstrated, by means of a specific methodology, that DECT performed at 80 and 140 kVp could assess liver iron and that there was a strong correlation amongst computational levels of iron (VIC) and LIC in rabbit models. In human studies, the same group found a strong correlation between LIC assessments based on MRI and VIC, indicating that DECT might be an equally valuable tool as MRI for determining iron content [33].

Fischer et al. [35] created virtual iron pictures using DECT, which made it possible to estimate iron levels accurately regardless of fat composition and liver tissue attenuation. With boundaries defined for various levels of iron overabundance these images exhibited astounding precision in determining LIC, suggesting DECT is a feasible approach for iron quantification. Even with the positive results, more testing versus liver biopsy is required to confirm VIC's validity, a reliable non-invasive technique for assessing liver iron in medical settings. Similarly, with the rise in hepatic steatosis linked to metabolic dysfunction, including alcoholic and non-alcoholic fatty liver disorders (NAFLD), non-invasive methods of assessing liver fat have gained popularity. At the moment, non-invasive techniques like MRI and MR spectroscopy are the most accurate ways to quantify liver fat content [36]. Single-energy CT is not devoid of drawbacks, though, particularly in the presence of iron. Because DECT can be employed to assess the hepatic fat percentage, research suggests that it has the potential to overcome these limitations [37, 38, 39].

DECT was utilized by Fischer et al. [35] to generate virtual non-iron images, allowing precise fat quantification regardless of the presence of iron. Artz et al. [41] have demonstrated a high correlation between tissue triglyceride ratios and histological fat scoring and DECT measurements in both laboratory animal models and human research. When comparing the quantification of iron and fat to the assessment of liver fibrosis using DECT, the latter is still in its infancy [43].

DECT therefore holds significant potential for application in neuroimaging, the detection of uric acid stones, and measuring of iron, fat, and fibrosis in the liver. Moreover, a number of promising investigations have demonstrated significant associations between DECT-derived measures and traditional methods such as MRI and biopsy. While further research is required to fully assess these techniques, DECT may potentially provide a helpful non-invasive alternative for imaging assessments and disease detection.

III. CONCLUSION

There are many uses for the Dual Energy Computed Tomography (DECT) method in the determination of illness. In this article, the DECT technology is first introduced. Second, the incorporation of DECT in neuroimaging and the diagnosis of illnesses such as stones made from uric acid and liver ailments are analyzed. DECT imaging is still being fully utilized in terms of its potential for disease identification. Future technological advancements may enable DECT's smooth incorporation into clinical practice and broaden the range of therapeutic benefits it offers.

REFERENCES

[1] T. R. Johnson, “Dual-energy CT: General Principles,” American Journal of Roentgenology, vol. 199, no. 5 Suppl., pp. S3–S8, Nov. 2012, doi: 10.2214/AJR.12.9116.

[2] M. Grasruck, S. Kappler, M. Reinwand, and K. Stierstorfer, “Dual Energy with Dual Source CT and kVp Switching with Single Source CT: A Comparison of Dual Energy Performance,” in Proceedings of SPIE, vol. 7258, 2009.

[3] K. E. Maturen, R. K. Kaza, P. S. Liu, L. E. Quint, S. H. Khalatbari, and J. F. Platt, “Sweet Spot for Endoleak Detection: Optimizing Contrast to Noise Using Low-keV Reconstructions from Fast-Switch kVp Dual-Energy CT,” Journal of Computer Assisted Tomography, vol. 36, pp. 83–87, 2012.

[4] P. M. Shikhaliev and S. G. Fritz, “Photon Counting Spectral CT Versus Conventional CT: Comparative Evaluation for Breast Imaging Application,” Physics in Medicine and Biology, vol. 56, pp. 1905–1930, 2011.

[5] D. P. Cormode, E. Roessl, A. Thran, et al., "Atherosclerotic Plaque Composition: Analysis with Multi-Color CT and Targeted Gold Nanoparticles," Radiology, vol. 256, pp. 774–782, 2010.
[6] S. Kappler, S. Hölzer, E. Kraft, K. Stierstorfer, and T. Flohr, "Quantum-Counting CT in the Regime of Count-Rate Paralysis: Introduction of the Pile-Up Trigger Method," in Proceedings of SPIE, vol. 7961, 2011.
[7] E. G. Hoeffner, S. K. Mukherji, A. Srinivasan, and D. J. Quint, "Neuroradiology Back to the Future: Spine Imaging," American Journal of Neuroradiology, vol. 33, pp. 999–1006, 2012, doi: 10.3174/ajnr.A3129.
[8] E. G. Hoeffner, S. K. Mukherji, A. Srinivasan, and D. J. Quint, "Neuroradiology Back to the Future: Brain Imaging," American Journal of Neuroradiology, vol. 33, pp. 5–11, 2012, doi: 10.3174/ajnr.A2936.
[9] R. A. Brooks, "A Quantitative Theory of the Hounsfield Unit and Its Application to Dual Energy Scanning," Journal of Computer Assisted Tomography, vol. 1, pp. 487–493, 1977, doi: 10.1097/00004728-197710000-00016.
[10] T. G. Flohr, C. H. McCollough, H. Bruder, et al., "First Performance Evaluation of a Dual-Source CT (DSCT) System," European Radiology, vol. 16, pp. 256–268, 2006, doi: 10.1007/s00330-005-2919-2.
[11] W. Bautz and W. A. Kalender, "Material Selective Imaging and Determination of Density Using the Dual Energy Method. II. Clinical Use of Dual Energy Radiography," Digitale Bilddiagnostik, vol. 7, pp. 95–103, 1987.
[12] W. Kalender, W. Bautz, D. Felsenberg, C. Suss, and E. Klotz, "Material-Selective Imaging and Density Measurement Using the Dual-Energy Method. I. Principles and Methodology," Digitale Bilddiagnostik, vol. 7, pp. 66–72, 1987.
[13] A. M. Tawfik, J. M. Kerl, R. W. Bauer, et al., "Dual-Energy CT of Head and Neck Cancer: Average Weighting of Low- and High-Voltage Acquisitions to Improve Lesion Delineation and Image Quality—Initial Clinical Experience," Investigative Radiology, vol. 47, pp. 306–311, 2011, doi: 10.1097/RLI.0b013e31821e3062.
[14] A. M. Tawfik, J. M. Kerl, A. A. Razek, et al., "Image Quality and Radiation Dose of Dual-Energy CT of the Head and Neck Compared with a Standard 120-kVp Acquisition," American Journal of Neuroradiology, vol. 32, pp. 1994–1999, 2011, doi: 10.3174/ajnr.A2654.
[15] A. M. Tawfik, A. A. Razek, J. M. Kerl, N. E. Nour-Eldin, R. Bauer, and T. J. Vogl, "Comparison of Dual-Energy CT-Derived Iodine Content and Iodine Overlay of Normal, Inflammatory and Metastatic Squamous Cell Carcinoma Cervical Lymph Nodes," European Radiology, vol. 24, pp. 574–580, 2014, doi: 10.1007/s00330-013-3035-3.
[16] A. Srinivasan, R. A. Parker, A. Manjunathan, M. Ibrahim, G. V. Shah, and S. K. Mukherji, "Differentiation of Benign and Malignant Neck Pathologies: Preliminary Experience Using Spectral Computed Tomography," Journal of Computer Assisted Tomography, vol. 37, pp. 666–672, 2013, doi: 10.1097/RCT.0b013e3182976365.
[17] M. Toepker, C. Czerny, H. Ringl, et al., "Can Dual-Energy CT Improve the Assessment of Tumor Margins in Oral Cancer?," Oral Oncology, vol. 50, pp. 221–227, 2014, doi: 10.1016/j.oraloncology.2013.12.001.
[18] A. E. Grams, J. Sender, R. Moritz, et al., "Dual Energy CT Myelography After Lumbar Osteosynthesis," Fortschritte auf dem Gebiet der Röntgenstrahlen und der Bildgebenden Verfahren, vol. 186, pp. 670–674, 2014, doi: 10.1055/s-0034-1373359.
[19] D. Morhard, L. Ertl, W. Gerdsmeier-Petz, B. Ertl-Wagner, and G. Schulte-Altedorneburg, "Dual-Energy CT Immediately After Endovascular Stroke Intervention: Prognostic Implications," Cardiovascular and Interventional Radiology, vol. 37, pp. 1171–1178, 2014.
[20] A. A. Postma, M. Das, A. A. Stadler, and J. E. Wildberger, "Dual-Energy CT: What the Neuroradiologist Should Know," Current Radiology Reports, vol. 3, no. 5, Art. no. 16, 2015, doi: 10.1007/s40134-015-0097-9.
[21] A. Graser, T. R. Johnson, M. Bader, et al., "Dual Energy CT Characterization of Urinary Calculi: Initial In Vitro and Clinical Experience," Investigative Radiology, vol. 43, pp. 112–119, 2008.
[22] D. T. Boll, N. A. Patil, E. K. Paulson, et al., "Renal Stone Assessment with Dual-Energy Multidetector CT and Advanced Postprocessing Techniques: Improved Characterization of Renal Stone Composition—Pilot Study," Radiology, vol. 250, pp. 813–820, 2009.
[23] P. Stolzmann, M. Kozomara, N. Chuck, et al., "In Vivo Identification of Uric Acid Stones with Dual-Energy CT: Diagnostic Performance Evaluation in Patients," Abdominal Imaging, vol. 35, pp. 629–635, 2010.
[24] P. Stolzmann, H. Scheffel, K. Rentsch, et al., "Dual-Energy Computed Tomography for the Differentiation of Uric Acid Stones: Ex Vivo Performance Evaluation," Urological Research, vol. 36, pp. 133–138, 2008.

[25] S. Li, A. H., J. M. Cardona, et al., "Dual-Energy CT for Quantification of Urinary Stone Composition in Mixed Stones: A Phantom Study," American Journal of Roentgenology, vol. 207, no. 2, 2016, doi: 10.2214/AJR.15.15692.

[26] D. Hernando, Y. S. Levin, C. B. Sirlin, *et al*., "Quantification of Liver Iron with MRI: State of the Art and Remaining Challenges," *Journal of Magnetic Resonance Imaging*, vol. 40, no. 5, pp. 1003–1021, 2014.

[27] C. B. Sirlin and S. B. Reeder, "Magnetic Resonance Imaging Quantification of Liver Iron," *Magnetic Resonance Imaging Clinics of North America*, vol. 18, no. 3, pp. 359–381, 2010.

[28] H. Chandarana, R. P. Lim, J. H. Jensen, *et al*., "Hepatic Iron Deposition in Patients with Liver Disease: Preliminary Experience with Breath-Hold Multiecho T2*-Weighted Sequence," *American Journal of Roentgenology*, vol. 193, no. 5, pp. 1261–1267, 2009.

[29] H. Ryden and M. Skorpil, "Quantification of Severe Liver Iron Overload Using MRI Offset Echoes," *Acta Radiologica Open*, vol. 4, no. 5, 2015.

[30] R. W. Chapman, G. Williams, G. Bydder, *et al*., "Computed Tomography for Determining Liver Iron Content in Primary Haemochromatosis," *British Medical Journal*, vol. 280, no. 6212, pp. 440–442, 1980.

[31] R. G. Sephton, "The Potential Accuracy of Dual-Energy Computed Tomography for the Determination of Hepatic Iron," *British Journal of Radiology*, vol. 59, no. 700, pp. 351–353, 1986.

[32] E. Joe, S. H. Kim, K. B. Lee, *et al*., "Feasibility and Accuracy of Dual-Source Dual-Energy CT for Noninvasive Determination of Hepatic Iron Accumulation," *Radiology*, vol. 262, no. 1, pp. 126–135, 2012.

[33] X. F. Luo, X. Q. Xie, S. Cheng, *et al*., "Dual-Energy CT for Patients Suspected of Having Liver Iron Overload: Can Virtual Iron Content Imaging Accurately Quantify Liver Iron Content?," *Radiology*, vol. 277, no. 1, pp. 95–103, 2015.

[34] X. F. Luo, Y. Yang, J. Yan, *et al*., "Virtual Iron Concentration Imaging Based on Dual-Energy CT for Noninvasive Quantification and Grading of Liver Iron Content: An Iron Overload Rabbit Model Study," *European Radiology*, vol. 25, no. 9, pp. 2657–2664, 2015.

[35] M. A. Fischer, C. S. Reiner, D. Raptis, *et al*., "Quantification of Liver Iron Content with CT: Added Value of Dual-Energy," *European Radiology*, vol. 21, no. 8, pp. 1727–1732, 2011.

[36] R. Kawata, K. Sakata, T. Kunieda, *et al*., "Quantitative Evaluation of Fatty Liver by Computed Tomography in Rabbits," *American Journal of Roentgenology*, vol. 142, no. 4, pp. 741–746, 1984.

[37] B. Y. Hur, J. M. Lee, H. W. Hyunsik, *et al*., "Quantification of the Fat Fraction in the Liver Using Dual-Energy Computed Tomography and Multi-Material Decomposition," *Journal of Computer Assisted Tomography*, vol. 38, no. 6, pp. 845–852, 2014.

[38] M. A. Fischer, R. Gnannt, D. Raptis, *et al*., "Quantification of Liver Fat in the Presence of Iron and Iodine: An Ex Vivo Dual-Energy CT Study," *Investigative Radiology*, vol. 46, no. 6, pp. 351–358, 2011.

[39] B. N. Patel, R. A. Kumbla, L. L. Berland, *et al*., "Material Density Hepatic Steatosis Quantification on Intravenous Contrast-Enhanced Rapid Kilovolt (Peak)-Switching Single-Source Dual-Energy Computed Tomography," *Journal of Computer Assisted Tomography*, vol. 37, no. 6, pp. 904–910, 2013.

[40] J. H. Li, C. Y. Tsai, and H. M. Huang, "Assessment of Hepatic Fatty Infiltration Using Dual-Energy Computed Tomography: A Phantom Study," *Physiological Measurement*, vol. 35, no. 4, pp. 597–606, 2014.

[41] N. S. Artz, C. D. Hines, S. T. Brunner, *et al*., "Quantification of Hepatic Steatosis with Dual-Energy Computed Tomography: Comparison with Tissue Reference Standards and Quantitative Magnetic Resonance Imaging in the ob/ob Mouse," *Investigative Radiology*, vol. 47, no. 10, pp. 603–610, 2012.

[42] X. Zheng, Y. Ren, W. T. Phillips, *et al*., "Assessment of Hepatic Fatty Infiltration Using Spectral Computed Tomography Imaging: A Pilot Study," *Journal of Computer Assisted Tomography*, vol. 37, no. 2, pp. 134–141, 2013.

[43] K. Hashimoto, T. Murakami, K. Dono, *et al*., "Assessment of the Severity of Liver Disease and Fibrotic Change: The Usefulness of Hepatic CT Perfusion Imaging," *Oncology Reports*, vol. 16, no. 4, pp. 677–683, 2006.

[44] M. Ronot, T. Asselah, V. Paradis, *et al*., "Liver Fibrosis in Chronic Hepatitis C Virus Infection: Differentiating Minimal from Intermediate Fibrosis with Perfusion CT," *Radiology*, vol. 256, no. 1, pp. 135–142, 2010.